Human Cytomegalovirus Infection of Tumor Cells Downregulates NCAM (CD56): A Novel Mechanism for Virus-Induced Tumor Invasiveness[1]

Roman A. Blaheta*, Wolf-Dietrich Beecken[†], Tobias Engl[†], Dietger Jonas[†], Elsie Oppermann[‡], Michael Hundemer*, Hans Wilhelm Doerr*, Martin Scholz* and Jindrich Cinatl Jr*

*Zentrum der Hygiene, Institut für Medizinische Virologie, Germany; [†]Zentrum der Chirurgie, Klinik für Urologie und Kinderurologie, Germany; [‡]Zentrum der Chirurgie, Klinik für Allgemein- und Gefäßchirurgie, Johann Wolfgang Goethe-Universität, Frankfurt am Main, Germany

Abstract

Pathologic data indicate that human cytomegalovirus (HCMV) infection might be associated with the pathogenesis of several human malignancies. However, no definitive evidence of a causal link between HCMV infection and cancer dissemination has been established to date. This study describes the modulation of the invasive behavior of NCAM-expressing tumor cell lines by HCMV. Neuroblastoma (NB) cells, persistently infected with the HCMV strain AD169 (UKF-NB-4[AD169] and MHH-NB-11[AD169]), were added to endothelial cell monolayers and adhesion and penetration kinetics were measured. The 140- and 180-kDa isoforms of the adhesion receptor NCAM were evaluated by flow cytometry, Western blot, and reverse transcription–polymerase chain reaction (RT-PCR). The relevance of NCAM for tumor cell binding was proven by treating NB with NCAM antisense oligonucleotides or NCAM transfection. HCMV infection profoundly increased the number of adherent and penetrated NB, compared to controls. Surface expression of NCAM was significantly lower on UKF-NB-4[AD169] and MHH-NB-11[AD169], compared to mock-infected cells. Western-blot and RT-PCR demonstrated reduced protein and RNA levels of the 140- and 180-kDa isoform. An inverse correlation between NCAM expression and adhesion capacity of NB has been shown by antisense and transfection experiments. We conclude that HCMV infection leads to downregulation of NCAM receptors, which is associated with enhanced tumor cell invasiveness.
Neoplasia (2004) **6**, 323–331

Introduction

Human cytomegalovirus (HCMV) is a β-herpes virus that persistently infects 50% to 90% of the adult population. Pathologic studies indicate that HCMV infection might be associated with the pathogenesis of several human malignancies. HCMV nucleic acids and proteins are present in a high percentage of low- and high-grade malignant gliomas, and expression of early and delayed HCMV gene products occurs in these tumors [1]. Recently, significant amounts of HCMV proteins and nucleic acids have been detected in prostate carcinoma lesions [2], and also found to be localized specifically in neoplastic cells in human colorectal polyps and adenocarcinomas [3].

The oncogenic potential of HCMV is well established *in vitro*. HCMV inhibits apoptosis [4], induces malignant transformation, and dysregulates key cellular pathways involved in mutagenesis, angiogenesis [5], and evasion of immune recognition [6].

However, although the abovementioned studies indicate that HCMV could facilitate tumor progression, there is still no definitive evidence of a causal link between HCMV infection and human cancer. One reason for this lack of evidence may be due to the limited availability of adequate cell culture models. HCMV-specific components are not detectable after long-term subcultures of tumor tissues [7]. Moreover, the presence of HCMV genetic information in human tumors is difficult to interpret because HCMV can infect these organs latently in a high percentage of normal individuals [8]. It also remains possible that HCMV modulates the biologic properties of malignant cells without being directly involved in carcinogenesis.

To elucidate the role of HCMV in tumor pathology *in vitro*, long-term infection was mimicked using persistently infected tumor cell lines [9]. Furthermore, we established an *in vitro* assay, which allows the separate analysis of tumor cells that adhere to an endothelial cell monolayer and those that transmigrate underneath the endothelium. We also considered adhesion molecule expression because surface receptors are

strongly implicated in tumor invasion. The neural cell adhesion molecule (NCAM; CD56) was chosen to be the representative molecule, as several data indicate that changes in NCAM expression play an essential part in the progression to tumor metastasis and that the modulation of NCAM is one rate-limiting event in the metastatic dissemination of tumor cells [10].

In the present study, NCAM-expressing neuroblastoma (NB) cells were employed as the model tumor. The invasive behavior of persistently infected NB cell lines has been evaluated and compared to the invasive capacity of noninfected variants. Analysis of the 140- and 180-kDa NCAM isoforms was included in this study, as well. This is the first report which demonstrates that HCMV directly contributes to augmented tumor cell adhesion and transendothelial penetration, and that this process is mediated through downregulation of NCAM.

Materials and Methods

Cell Cultures

Human umbilical vein endothelial cells (HUVECs) were harvested by enzymatic treatment with chymotrypsin. HUVECs were grown in Medium 199 (M199; Biozol, Munich, Germany) and supplemented with 10% fetal calf serum (FCS), 10% pooled human serum, 20 μg/ml endothelial cell growth factor (Boehringer, Mannheim, Germany), 0.1% heparin, 100 ng/ml gentamicin, and 20 mM Hepes buffer (pH 7.4). Subcultures from passages 2 to 4 were selected for experimental use. The NB cell line UKF-NB-4 was established from bone marrow metastasis of Evans stage 4 NB [11]. The NB cell line MHH-NB-11 was purchased from DSMZ (Braunschweig, Germany). NB cells were grown and subcultured in Iscove's modified Dulbecco's medium (IMDM; Seromed, Berlin, Germany) supplemented with 10% FCS, 100 IU/ml penicillin, and 100 μg/ml streptomycin at 37°C in a humidified 5% CO_2 incubator.

Establishment of Persistent HCMV Infection

HCMV laboratory strain AD169 was purchased from ATCC (Rockville, MD). Virus stock was prepared in human foreskin fibroblast (HFF) incubated in MEM, supplemented with 4% FBS. Virus titer was determined by plaque titration in HFF cells, as described previously [11]. NB cells were infected with HCMV at a multiplicity of infection of 10. After virus adsorption for 60 to 90 minutes at 37°C, cells were incubated for 22 days and then split at a ratio of 1:5. Subcultures were split at a ratio of 1:3 at 8-day intervals. Cells were designated UKF-NB-4[AD169] and MHH-NB-11[AD169]. Immunoperoxidase staining against the HCMV-specific immediate early protein (72-kDa immediate early Ag IEA, UL123; DuPont, Bad Homburg, Germany) or the nuclear late protein (67 kDa late Ag; LA; DuPont) was carried out routinely after each subculture [12]. The efficiency of HCMV infection was always about 30%, related to IEA-expressing cells (see further details in Results section). For control purposes, an irrelevant antibody directed against

HSV glycoprotein B was used. Mock-infected inocula were prepared in an identical fashion, except that NB cells were not infected with HCMV.

Monolayer Invasion Assay

Round cover slips were treated with 3-aminopropyl-triethoxy-silan (2%; Sigma, München, Germany)–acetone solution for 60 minutes (20°C) to allow firm adhesion of HUVECs and placed into six-well multiplates (Falcon Primaria; Becton Dickinson, Heidelberg, Germany). HUVEC subcultures were transferred to prepared multiplates in complete HUVEC medium. When confluency was reached, 0.5×10^6 NB/well was carefully added to the HUVEC monolayer for various time periods. Subsequently, nonadherent NB cells were washed off using warmed (37°C) M199. The remaining cells were fixed with 1% glutaraldehyde. Bound NB cells were counted in five different fields (5×0.25 mm^2) using a phase-contrast microscope ($\times 20$ objective) and the mean cellular adhesion rate was calculated.

To separately assess NB cells that had penetrated the HUVEC monolayer, a reflection interference contrast microscope with a Ploem apparatus was used. The relevant theoretical evaluation of reflection contrast microscopy is given by Bereiter-Hahn et al. [13] and Gingell and Todd [14]. The resulting images were visualized and amplified by a Proxitronic CCD camera (Proxitronic, Bensheim, Germany). The number of penetrated NB was then quantified using the image analyzing system ARGUS 20 (Hamamatsu, Hersching, Germany). To optimize the signal-to-noise ratio, online background subtraction and averaging of eight images were performed, using the image processing system QUANTI-MET Q520 (Cambridge Instruments, Bensheim, Germany). Cells that penetrated the HUVEC monolayer were counted in five different fields (5×0.25 mm^2, $\times 20$ objective), and mean penetration rate was calculated as percentage of all cells added.

Cell Proliferation

Proliferative activity of NB cells and HUVECs was estimated by the PicoGreen (MoBiTec, Goettingen, Germany) assay as described elsewhere [15]. Briefly, at several time points after plating the cells in six-well multiplates, the culture medium was removed and cells were digested with papain (0.125 mg/ml protein) for 20 hours at 60°C. Thereafter, the fluorescent dye PicoGreen, which shows high specificity for dsDNA, was added (1:200 dilution) for 10 minutes at 20°C. Fluorescence intensity was determined using a computer-controlled fluorescence reader (Cytofluor 2300 plate scanner; Millipore, Eschborn, Germany) at $\lambda_{ex} = 485$ nm and $\lambda_{em} = 530$ nm.

Evaluation of NCAM Surface Expression

NB cells were disaggregated mechanically, washed in blocking solution (phosphate-buffered saline [PBS], 0.5% BSA), and then incubated for 60 minutes at 4°C with an fluorescein isothiocyanate (FITC)–conjugated monoclonal antibody anti- CD56, which detects the NCAM 140- and

180-kDa isoform (clone ERIC-1). NCAM expression of NB cells was then measured using a FACscan (FL-1H [log] channel histogram analysis; 1×10^4 cells/scan; Becton Dickinson) and expressed as relative fluorescence units (RFU).

To determine if NCAM modulation was restricted to HCMV-infected NB cells, NB cultures were double-stained using an FITC-conjugated anti−CD56 monoclonal antibody and the monoclonal antibody directed against the HCMV-specific 72-kDa IEA, which was coupled to indocarbocyanine (Cy3; Dianova, Hamburg, Germany). At first, cells were fixed with 100 μl of fixation medium (Fix and Perm; Biozol-An der Grub Bioresearch, Eching, Germany) and washed twice in blocking solution (PBS, 0.5% BSA). Subsequently, they were incubated for 60 minutes at 4°C with 100 μl of permeabilization medium (Fix and Perm) together with the monoclonal antibody anti−72-kDa IEA. This process was repeated to allow Cy3 labeling. In a further step, NB cells were marked with the FITC-conjugated anti−CD56 monoclonal antibody. Dot plot quadrant analyses have been carried out to display percentage distribution of NB-expressing Cy3-IEA and/or FITC-NCAM (IEA$^+$/NCAM$^+$, IEA$^+$/NCAM$^-$, IEA$^-$/NCAM$^+$, IEA$^-$/NCAM$^-$). IEA$^-$ and IEA$^+$ cells were gated to obtain two distinct cell populations: population I (IEA$^+$) as HCMV-infected cells and population II (IEA$^-$) as noninfected NB cells. NCAM expression of both NB subtypes was then detected by FACscan analysis (FL-1H [log] channel histogram analysis; 1×10^4 cells/scan). A mouse IgG1-FITC was used as an isotype control for CD56 mouse IgG1-FITC−conjugated antibody. To evaluate background staining of Cy3-conjugated anti−72-kDa IEA, goat anti−mouse IgG Cy3 was used.

Western Blot Analysis

Total NCAM content in NB cells was evaluated by Western blot analysis: NB lysates were applied to a 7% polyacrylamide gel and electrophoresed for 90 minutes at 60 V. The protein was then transferred to nitrocellulose membranes. After blocking, the membranes were incubated overnight with the anti−NCAM antibody (dilution 1:1000). In additional experiments, the AB-1 monoclonal antibody was used (1:100; Calbiochem, Bad Soden, Germany) to detect *N-myc*. p73 was measured using monoclonal anti-p73 (clone ER-15, 1:500; Sigma). To identify ΔNp73, the monoclonal antibody anti-ΔNp73 (clone 38C674, 1:500) was purchased from Active Motif (Rixensart, Belgium). HRP-conjugated goat anti−mouse IgG (dilution 1:5000; Upstate Biotechnology, Lake Placid, NY) served as the secondary antibody. The membrane was briefly incubated with ECL detection reagent (ECL; Amersham, Freiburg, Germany) to visualize the proteins and exposed to an X-ray film (Hyperfilm EC; Amersham).

Reverse Transcription−Polymerase Chain Reaction (RT-PCR)

Total RNA was extracted and purified with Trizol reagent according to the manufacturer's instructions and treated with RNase-free DNase. The NCAM primer sequences were as follows: for NCAM-180: 5′-CGAGGCTGCCTCCGTCAGCACC-3′ and 5′-CCGGATCCATCATGCTTTGCTCTCG-3′; for NCAM-140: 5′-GAACCTGATCAAGCAGGATGACGG-3′ and 5′-CCGGATCCATCATGCTTTGCTCTCG-3′. Internal controls for the RT-PCR reaction were performed by running parallel reaction mixtures with the housekeeping gene *GAPDH*: 5′-ATCTTCCAGGAGCGAGATCC-3′ and 5′-ACCACTGACACGTTGGCAGT-3′. RNA (1−10 μg) was reverse-transcribed and the resulting cDNA was directly added to the PCR. Amplification reactions (20 μl) were performed in the presence of 1/10 (2 μl) of the cDNA reaction, with an initial incubation step at 94°C for 1 minute. Cycling conditions consisted of denaturation at 94°C for 1 minute, annealing at 55°C for 1 minute, and extension at 72°C for 1 minute over a total of 30 cycles. The reaction was completed by another incubation step at 72°C for 10 minutes. The PCR products were subjected to electrophoresis in 2% agarose gel and visualized by ethidium bromide.

Transfection Procedure

UKF-NB-4^{AD169} cells were transfected using the calcium phosphate coprecipitation method with full-length cDNA, encoding the human NCAM-140-kDa isoform inserted in sense of the eukaryotic expression vector pHβ-Apr-1-neo [16]. Control cells were transfected with the expression vector alone. A total of 0.5×10^6 NB was seeded in 25-cm^2 culture flasks, grown overnight, and transfected with 2 μg of DNA. After culturing for 16 hours in complete medium, cells were washed twice with PBS without Ca^{2+} and Mg^{2+} and then incubated with fresh cell culture medium. Twenty-four hours after transfection, NCAM expression was assayed by FACS analysis and adhesion experiments were carried out. NB cell populations were not further sorted prior to the assay. Efficiency of NCAM transfection using pHβ-Apr1-neo was investigated fluorometrically by calcium phosphate coprecipitation of pHβ-Apr1-neo in combination with pEGFP-N1 vector (Clontech GmbH, Heidelberg, Germany) at a ratio of 1:1. pEGFP-N1 encodes a red-shifted variant of wild-type GFP, which has been optimized for brighter fluorescence and higher expression in mammalian cells. Fluorescence analysis revealed a transfection rate of pHβ-Apr1-neo of 30%. Viability of the cells, which was controlled by trypan blue dye exclusion or quantitative fluorescence analysis of propidium iodide uptake, was >90%.

Oligonucleotide Treatment of NB

In control studies, subconfluent parental UKF-NB-4 cells were treated with NCAM antisense phosphorothioate oligonucleotides and CG-matched randomized sequence phosphorothioate oligonucleotides, whose sequences are CAT GGC TAC GCA CC (NCAM antisense) and ACC GAC CGA CGT GT (random antisense). The antisense oligonucleotides and controls were designed and manufactured by Biognostic (Göttingen, Germany). Cells were washed three times in prewarmed PBS. A total of 100 μg/ml of oligonucleotides was premixed for 10 minutes with 30 μg/ml DOTAP liposomal transfection reagent (Boehringer) in 70 μl of Hepes buffer (1:10 in PBS) and the desired concentration of 1 μg/ml was applied to washed cells. NB cells were incubated with the
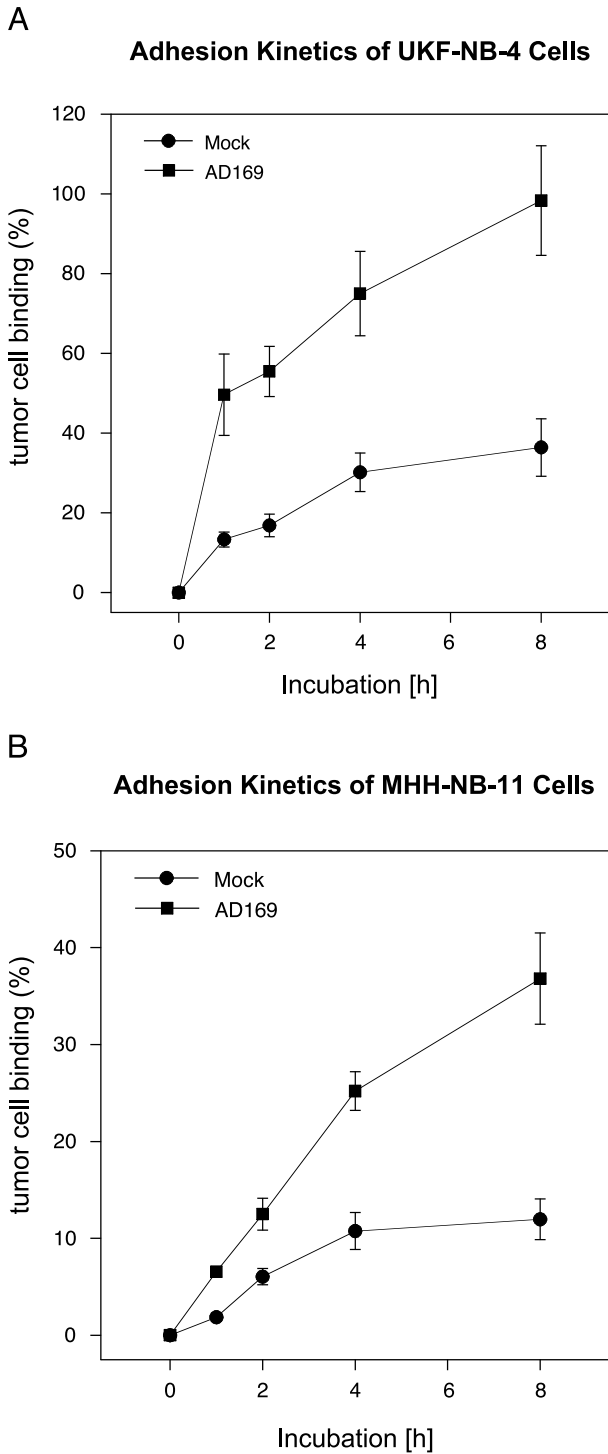
A

Adhesion Kinetics of UKF-NB-4 Cells

B

Adhesion Kinetics of MHH-NB-11 Cells

Figure 1. *Adhesion kinetics of UKF-NB-4^{AD169} (A) and MHH-NB-11^{AD169} (B) versus mock-infected controls. NB cells were added at a density of 0.5×10^6 cells/well to HUVEC monolayers for different time periods. Non-adherent tumor cells were washed off in each sample, and the remaining cells were fixed and counted in five different fields (5×0.25 mm^2) using a phase-contrast microscope. Adhesion capacity is depicted as tumor cell binding and given in percentage of all cells added (mean ± SD; n = 5). X-axis indicates the period of coculture.*

oligonucleotides for 24 hours at 37°C, after which the medium was removed and replaced with standard growth medium for another 24 hours. To confirm that oligonucleotides could penetrate NB cells, cells were treated with FITC-

labeled oligonucleotides, fixed after treatment with 0.5% formaldehyde, and analyzed by fluorescence microscopy. NCAM expression was measured by FACscan analysis. Cell viability was examined as mentioned above.
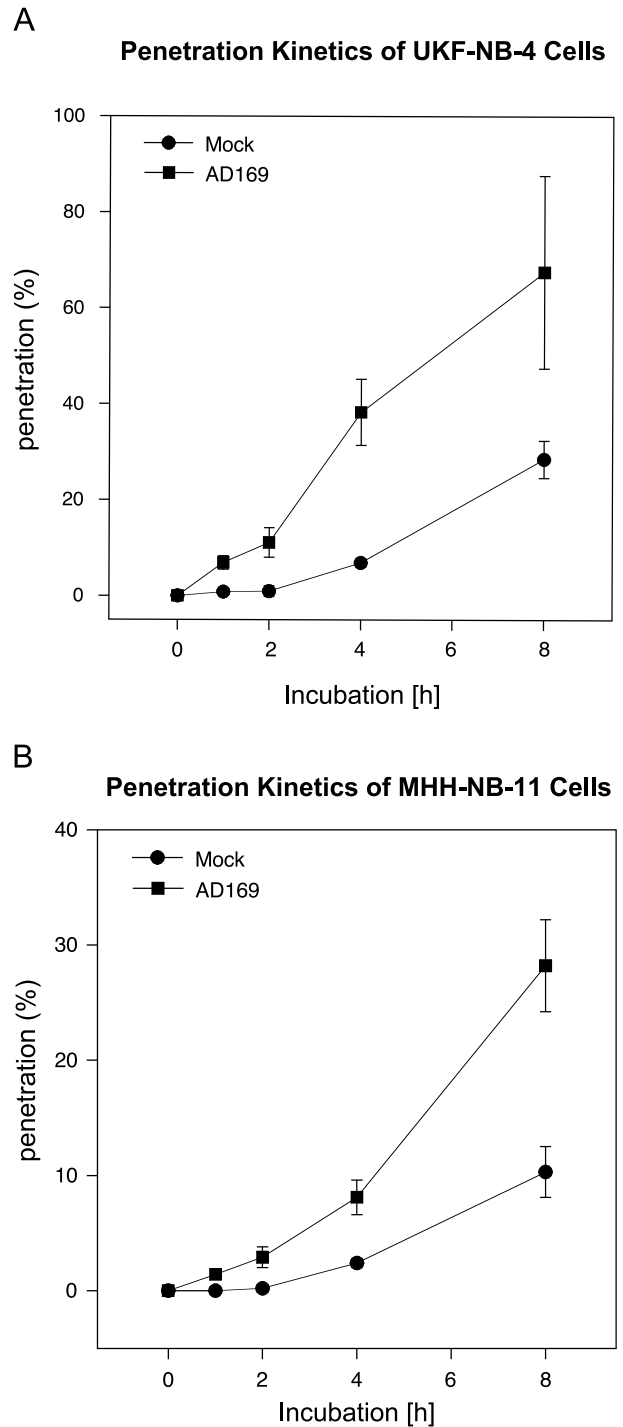
A

Penetration Kinetics of UKF-NB-4 Cells

B

Penetration Kinetics of MHH-NB-11 Cells

Figure 2. *Penetration kinetics of UKF-NB-4^{AD169} (A) and MHH-NB-11^{AD169} (B) versus mock-infected controls. NB cells were added at a density of 0.5×10^6 cells/well to HUVEC monolayers for different time periods. To identify transmigrated NB from the cells which had bound to HUVEC, a reflection interference contrast microscope with a Ploem apparatus was used (see Materials and Methods section for details). Five different observation fields (5×0.25 mm^2) were chosen and mean penetration rate was evaluated in each sample. Penetration rate is given as percentage of all cells added (mean ± SD; n = 3). X-axis indicates the period of coculture.*
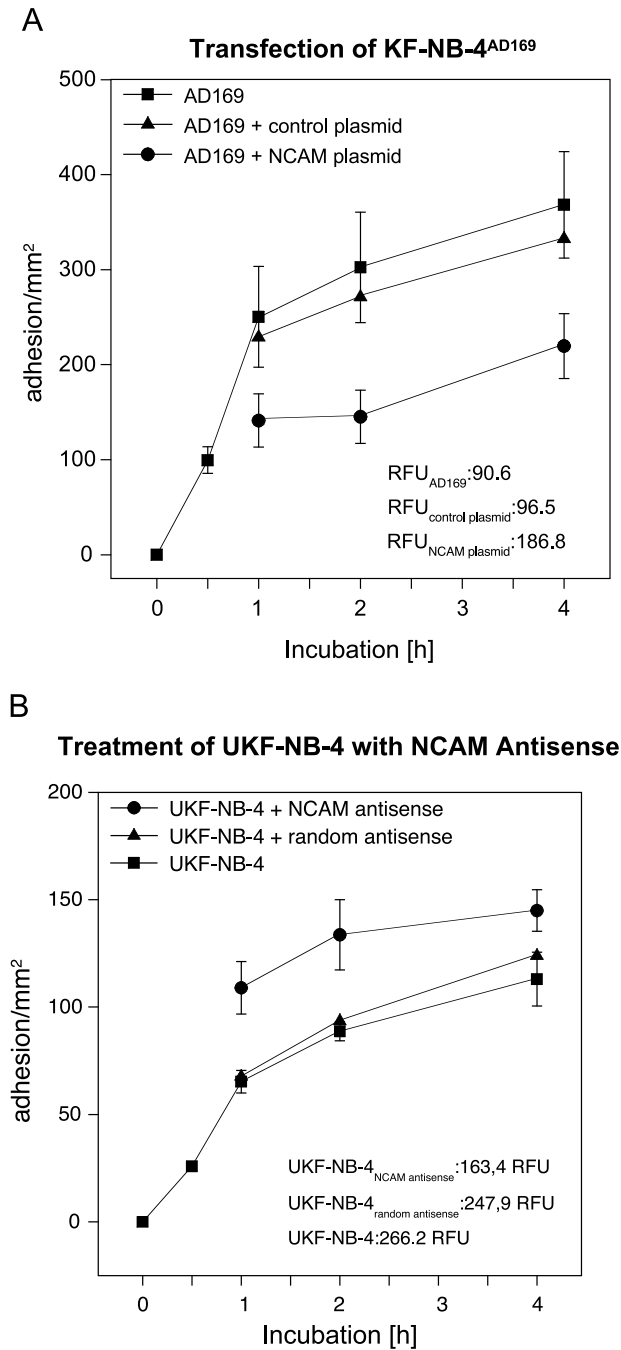
A

Transfection of KF-NB-4^{AD169}

- ■ AD169
- ▲ AD169 + control plasmid
- ● AD169 + NCAM plasmid

RFU$_{AD169}$:90.6
RFU$_{control\ plasmid}$:96.5
RFU$_{NCAM\ plasmid}$:186.8

B

Treatment of UKF-NB-4 with NCAM Antisense

- ● UKF-NB-4 + NCAM antisense
- ▲ UKF-NB-4 + random antisense
- ■ UKF-NB-4

UKF-NB-4$_{NCAM\ antisense}$:163,4 RFU
UKF-NB-4$_{random\ antisense}$:247,9 RFU
UKF-NB-4:266.2 RFU

Figure 3. *Graph (A) shows adhesion kinetics of UKF-NB-4^{AD169} transfected with 2 µg of full-length cDNA encoding the human NCAM-140-kDa isoform. Graph (B) demonstrates adhesion kinetics of parental UKF-NB-4 cells treated with 1 µg/ml NCAM antisense oligonucleotides. Control cells remained untreated or were either incubated with random antisense oligonucleotides or transfected with the expression vector alone. In all experiments, NB cells were added at a density of 0.5 × 10^6 cells/well to HUVEC monolayers. Nonadherent tumor cells were washed off after different time periods, and the remaining cells were fixed and counted in five different fields (5 × 0.25 mm^2) using a phase-contrast microscope. Data on NCAM surface expression, evaluated by flow cytometry, are also given in the lower right-hand corner and demonstrate the inverse correlation between NCAM expression level and adhesion capacity. X-axis indicates the period of coculture (mean ± SD, n = 3).*

Statistics

All experiments were carried out at least three times. Mean ± SD were calculated to produce the figures shown.

Statistical significance was determined by the Wilcoxon signed rank test showing two-sided probabilities and using normal approximation. Differences were considered statistically significant at a *P* value less than .05.

Results

Infiltration Kinetics of UKF-NB-4^{AD169} and MHH-NB-11^{AD169}

Figure 1 shows the adhesion kinetics of UKF-NB-4^{AD169} (Figure 1*A*) and MHH-NB-11^{AD169} (Figure 1*B*) *versus* mock-infected cells. The number of adherent UKF-NB-4 cells increased after 60 minutes (66.5±9.3 cells/mm^2) and
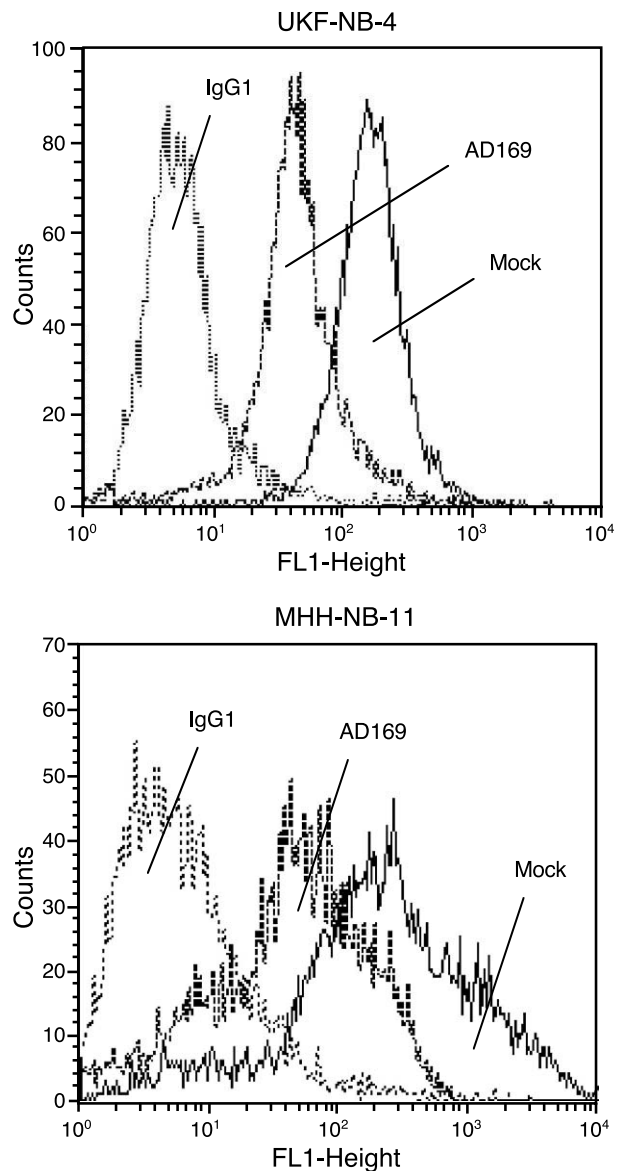

Figure 4. *NCAM surface expression on UKF-NB-4 (top) and MHH-NB-11 cells (bottom). Tumor cells were disaggregated mechanically and washed in blocking solution. An FITC-conjugated monoclonal antibody anti-CD56, clone ERIC-1, was used to detect the NCAM 140- and 180-kDa isoform. A mouse IgG1-FITC served as the isotype control (IgG1). "AD169" depicts HCMV-infected cells; "Mock" is related to mock infected controls. Fluorescence was analyzed using a FACScan flow cytometer, and a histogram plot (FL1-Height) was generated to show FITC fluorescence.*

A

UKF-NB-4

B

MHH-NB-11
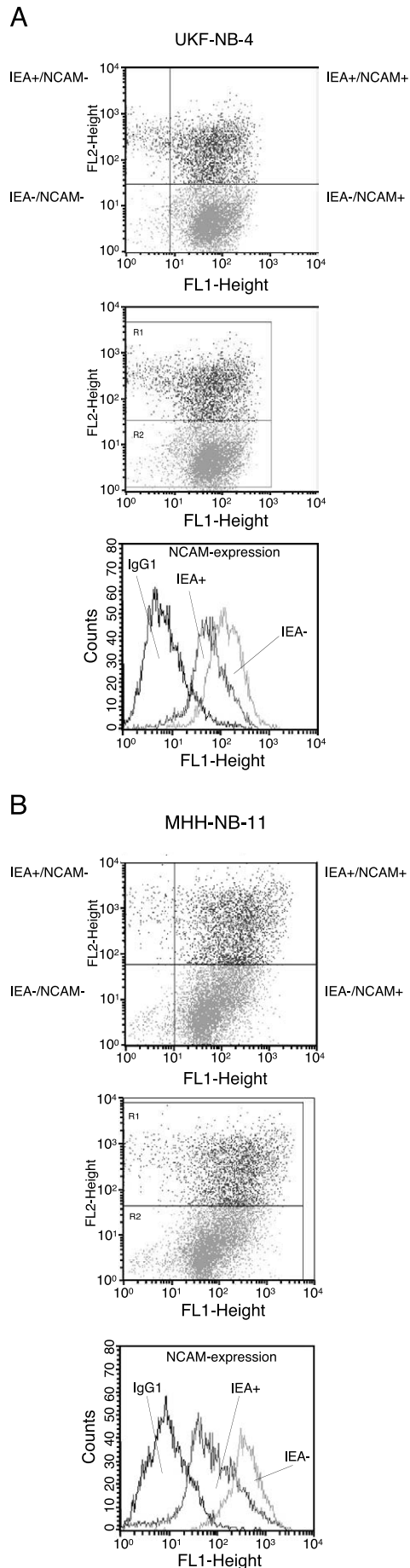
reached a plateau after 4 hours (150.9 ± 24.3 cells/mm^2). HCMV infection led to considerable enhancement of the adhesion process. The 60-minute adhesion values were 248.2 ± 51.5 cells/mm^2. A total of 491.6 ± 68.7 cells/mm^2 was adherent after 8 hours. The same was true for MHH-NB-11 cells. HCMV infection elevated the amount of adherent cells three-fold (60-minute values: MHH-NB-11: 9.3 ± 2.1 cells/mm^2; MHH-NB-11^{AD169}: 32.8 ± 2.7 cells/mm^2; 8-hour values: MHH-NB-11: 59.8 ± 10.6 cells/mm^2; MHH-NB-11^{AD169}: 183.9 ± 23.8 cells/mm^2). The same phenomenon was observed with NB cells, which penetrated underneath the HUVEC monolayer (Figure 2). The transmigration rates of both UKF-NB-4^{AD169} (Figure 2A) and MHH-NB-11^{AD169} (Figure 2B) were significantly upregulated, compared to transmigration of mock-infected controls. The PicoGreen assay, which had been carried out as well, revealed no proliferative activity of NB cells during this time.

NCAM Is Relevant for NB Cell Adhesion

The relevance of NCAM for tumor cell binding to HUVECs was demonstrated by transfection and antisense experiments. Transfection of UKF-NB-4^{AD169} cells with NCAM cDNA reverted the virus-evoked downregulating effect on this receptor and resulted in a two-fold enhancement of NCAM on the cellular membrane. Viability of UKF-NB-4^{AD169} was not affected by this procedure. Adhesion of transfected UKF-NB-4^{AD169} to HUVECs was strongly reduced ($P < .05$), compared to nontransfected cells (Figure 3A). Transfection of UKF-NB-4^{AD169} with a control plasmid did not change NCAM expression or cell attachment.

Treatment of parental UKF-NB-4 cells with NCAM antisense oligonucleotides diminished NCAM by 40% (viability >90%) and significantly enhanced tumor cell adhesion to HUVECs (Figure 3B). Control experiments using random antisense treated NB showed no difference to untreated NB.

HCMV Infection Leads to Reduced NCAM Expression

Surface expression of NCAM on UKF-NB-4^{AD169} and MHH-NB-11^{AD169} cells was strongly reduced compared to the NCAM level on mock-infected cells. Mean values of five experiments revealed 242.6 ± 49.2 RFU (UKF-NB-4^{Mock}) *versus* 101.9 ± 36.4 RFU (UKF-NB-4^{AD169}), or 562.1 ± 73.5

Figure 5. *Two-color fluorescence analysis of HCMV-infected UKF-NB-4 (A) and MHH-NB-11 cells (B). At first, UKF-NB-4^{AD169} (Figure 4, top) or MHH-NB-11^{AD169} cell cultures (Figure 4, bottom) were fixed and washed twice in blocking solution. Subsequently, they were incubated for 60 minutes at 4°C with permeabilization medium, together with the monoclonal antibody directed against the HCMV-specific 72-kDa IEA (UL123), which was then coupled to Cy3 indocarbocyanine. In the second step, NB cells were marked with the FITC-conjugated anti–CD56 monoclonal antibody (see Materials and Methods section for details). Dot plot quadrant analyses have been carried out to display percentage distribution of NB-expressing Cy3-IEA and/ or FITC-NCAM (IEA$^+$/NCAM$^+$, IEA$^+$/NCAM$^-$, IEA$^-$/NCAM$^+$, IEA$^-$/NCAM$^-$ — upper diagram). IEA$^+$ (R1) and IEA$^-$ (R2) cells were gated (middle diagram) to mark two distinct cell populations: population I (IEA$^+$) as HCMV-infected cells and population II (IEA−) as noninfected NB cells. Mean fluorescence intensity of NCAM expression of both NB subtypes was then detected by FACscan analysis (FL-1H [log] channel histogram analysis; 530 nm peak fluorescence [lower diagram]).*

RFU (MHH-NB-11^{Mock}) *versus* 278.4 ± 54.3 RFU (MHH-NB-11^{AD169}). Figure 4 shows the histogram analysis of one representative experiment.

Tumor cells can be subcultured continuously after initiation of infection, without losing the virus. This long-term persistence of virus in the tumor cell cultures is based on the balance between CMV-infected and noninfected tumor cells (i.e., between virus replication/release and proliferation of noninfected cells) [11]. To ensure that NCAM reduction was specifically restricted to the subset of HCMV-infected NB cells, a double-staining procedure was performed. Analysis of HCMV-infected tumor cell cultures demonstrated 30.92 ± 4.82% IEA$^+$ MHH-NB-11 cells (mean ± SD, n = 3), or 32.03 ± 5.31% IEA$^+$ UKF-NB-4 cells (mean ± SD, n = 3). Separate evaluation of both cell populations revealed that NCAM surface expression on IEA$^+$ cells is significantly lowered compared to the subset of noninfected IEA$^-$ cells. One representative experiment is shown in Figure 5, *A* and *B*.

NCAM Loss Is Paralleled by N-myc Increase, ΔNp73 Increase, and p73 Reduction

Further experiments were carried out using MHH-NB-11 cells. Western blot data presented evidence that both the NCAM 140- and 180-kDa proteins were reduced in HCMV-infected cell cultures, compared to mock-infected cells (Figure 6). Assessment of RNA expression of NCAM showed downmodulation of mRNA encoding the 140- and 180-kDa isoform (Figure 7). To get more insights into HCMV-
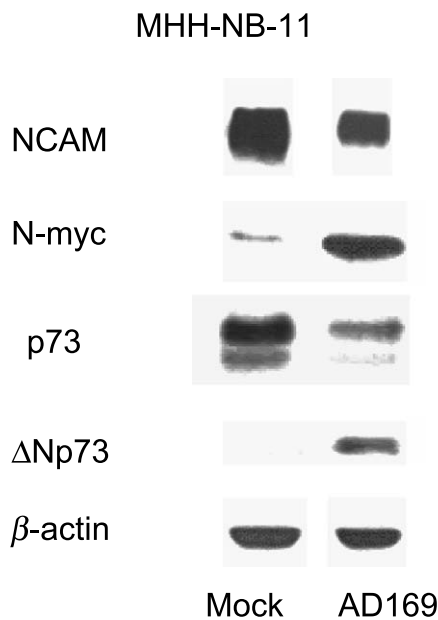
MHH-NB-11

Figure 7. *RT-PCR analysis of NCAM 140- and 180-kDa RNA in MHH-NB-11^{AD169} cells (AD169) versus mock-infected controls (mock). RNA were extracted, reverse-transcribed, and submitted to semiquantitative RT-PCR using gene-specific primers as indicated in Materials and Methods section. The figure shows one representative from three separate experiments.*

triggered tumorigenesis and NCAM regulation, respectively, the oncoprotein *N-myc*, the tumor-suppressor protein p73, and the truncated p73 isoform ΔNp73 were analyzed as well. Figure 6 demonstrates that both *N-myc* and ΔNp73 were drastically upregulated, whereas p73 was strongly reduced in HCMV-infected MHH-NB-11 cells compared to mock-infected controls. The same results were obtained from UKF-NB-4 *versus* UKF-NB-4^{AD169} cells (data not shown).

Discussion

Although there is evidence that infection with HCMV is clinically associated with enhanced tumor metastasis and progression, no clear data show that HCMV drives tumor cell invasion. So far, disordered migration of virus-infected neuronal cells has been observed in developing mouse brains after infection with murine cytomegalovirus [17,18]. In another experimental model, HCMV infection of smooth muscle cells (SMCs) has been linked to a significant increase of SMC migration. This migration was inhibited by the presence of anti–HCMV-neutralizing antibodies [19,20]. Scholz et al. [21] reported that adhesion of HCMV-infected NB cells, but not of noninfected control cells, resulted in focal disruption of the integrity of HUVEC monolayers, which then facilitated tumor cell transmigration. We present that HCMV directly contributes to augmented NB cell adhesion and transendothelial penetration, and that this process is mediated through downregulation of NCAM on tumor cells.

Several studies demonstrate the important role of NCAM in tumor migration and metastasis, with an inverse relationship between migratory potential of the cells and NCAM expression. In primitive neuroectodermal tumor cells, an increase in NCAM was paralleled by a significant reduction in cellular motility and adhesion capacity [22,23]. In a rat model, NCAM-transfected glioma tumor cells became less invasive and destructive than control cells

MHH-NB-11

Figure 6. *Western blot analysis of NCAM, N-myc, p73, and ΔNp73 from the proteins of MHH-NB-11 cells. MHH-NB-11 cells were either mock-infected or permanently infected with HCMV strain AD169. Cell lysates were subjected to sodium dodecyl sulfate polyacrylamide gel electrophoresis (SDS-PAGE) and blotted on the membrane incubated with anti–NCAM (clone ERIC-1), anti–N-myc (clone AB-1, anti–p73 (clone ER-15), or anti–ΔNp73 (clone 38C674) monoclonal antibodies. β-Actin served as the internal control. The figure shows one representative from three separate experiments.*
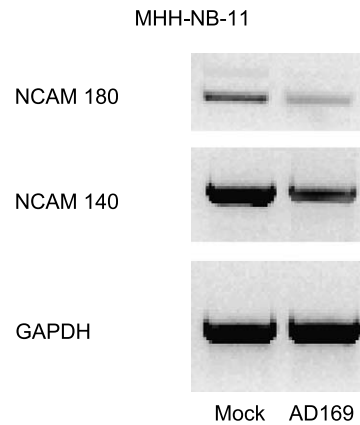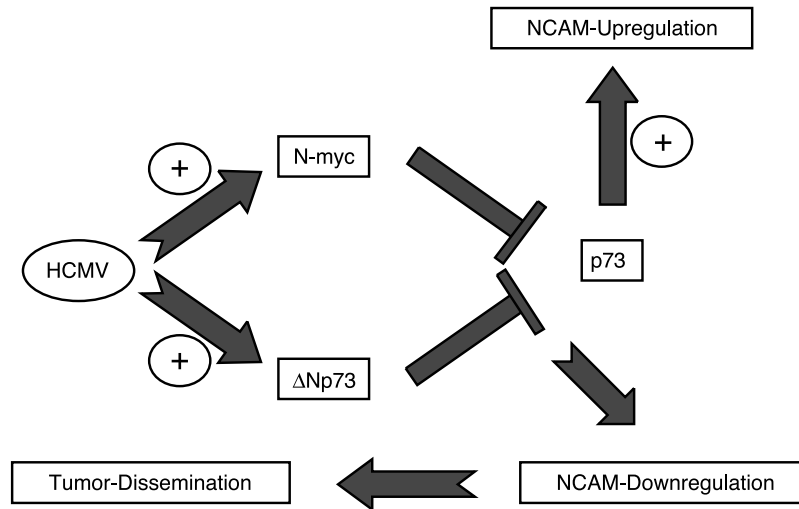
Figure 8. *Schematic model of HCMV-triggered tumor dissemination. HCMV amplifies both N-myc and ΔNp73. Overexpression of the ΔNp73 isoform generates a functional block of p73, with the net effect of NCAM downregulation. Loss of NCAM is strongly associated with enhanced tumor transmigration (see text for further details).*

with a low NCAM expression level [24]. Diminished expression of NCAM was also associated with clinically aggressive colon cancers [25–27], and dissemination of pancreatic β tumor cells [28,29]. Tezel et al. [30] concluded from their studies that NCAM expression in tubular adenocarcinoma of the pancreas has a significant impact on overall patient survival. It is currently assumed that NCAM, in its function as a homophilic receptor, stabilizes the primary tumor or tumor cell aggregates while circulating in the blood vessels. Reduction of the NCAM expression level might lead to a reduction in cell–cell binding forces, and hence to the release of tumors as single cells. The less NCAM, the more putative metastatic cells leave the tumor mass, and the more penetration events can take place [10].

Our data reveal strong upregulation of the oncoprotein *N-myc* in HCMV-infected cell cultures. Interestingly, NCAM expression is closely correlated to the *N-myc* oncogene level: transfection of the rat NB cell line B104 with an *N-myc* expression vector resulted in a dramatic reduction in the levels of NCAM polypeptides and mRNA and increased metastatic ability. Spontaneous revertants of the high *N-myc* phenotype were found to have regained significant levels of NCAM expression, indicating that the continued expression of *N-myc* is required to maintain the low NCAM phenotype [31]. Subsequent experiments on human NB cell lines have confirmed that *N-myc* regulates the expression of NCAM and that a reduced NCAM level is responsible for the outcome of enhanced tumorigenic properties [32,33]. In good accordance to our results, *N-myc* expression significantly increased in NB cells persistently infected with HCMV [11]. These findings clearly corroborate our hypothesis of HCMV-driven NCAM regulation and the involvement of *N-myc* in this process.

Recently, a homologue of the tumor-suppressor p53, termed p73, was described [34]. ΔNp73, an isoform of p73

lacking the N-terminal transactivation domain, was shown to create a dominant-negative feedback loop that regulates p73 function. Melino et al. [35] proposed that dysregulation of p73 and enhanced expression of ΔNp73 forms are associated with cancer development. Indeed, accumulation of ΔNp73 variants and loss of p73 full-length proteins have been found in human neuroblastic tumors [36]. ΔNp73 expression significantly correlated with poor overall and progression-free survival [37]. Interestingly, *in vitro* experiments demonstrated that transfected full-length p73 cDNA induces expression of NCAM and downregulation of *N-myc* in NB cells. Induction of differentiation by retinoids in the same NB cells was accompanied by accumulation of p73 and p73-regulated transactivation of the NCAM promoter. Inversely, transfection of dominant-negative p73 in NB cells abrogated the transactivation of the NCAM promoter induced by retinoids [38]. Meanwhile, it has been discovered that the *N-myc* gene directly modulates expression of p73/ΔNp73 and downstream elements [39].

The link between ΔNp73 gene products and viral infection was established by Allart et al. [40]. They observed a robust accumulation and stabilization of ΔNp73 in HCMV-infected NB cells, which was accompanied by a higher tumorigenicity, compared to mock-infected cells. Based on our *in vitro* model, we present evidence that long-term HCMV infection is accompanied by a loss of NCAM and p73, together with an increase of *N-myc* and ΔNp73. We therefore postulate a direct association between HCMV infection and tumor progression. HCMV shares the capacity of upregulating *N-myc* and ΔNp73. Interference in the *N-myc*/ΔNp73 signalling system causes, as at least one consequence, distinct downregulation of NCAM biosynthesis and receptor processing. NCAM loss finally attributes to the enhanced invasive capacity of tumor cells (Figure 8). Further studies should explore the effects of an antiviral therapy on tumor growth and dissemination *in vivo*.

Acknowledgement

References

[1] Cobbs CS, Harkins L, Samanta M, Gillespie GY, Bharara S, King PH, Nabors LB, Cobbs CG, and Britt WJ (2002). Human cytomegalovirus infection and expression in human malignant glioma. *Cancer Res* **62**, 3347–3350.

[2] Samanta M, Harkins L, Klemm K, Britt WJ, and Cobbs CS (2003). High prevalence of human cytomegalovirus in prostatic intraepithelial neoplasia and prostatic carcinoma. *J Urol* **170**, 998–1002.

[3] Harkins L, Volk AL, Samanta M, Mikolaenko I, Britt WJ, Bland KI, and Cobbs CS (2002). Specific localisation of human cytomegalovirus nucleic acids and proteins in human colorectal cancer. *Lancet* **360**, 1557–1563.

[4] Cinatl J Jr, Cinatl J, Vogel JU, Kotchetkov R, Driever PH, Kabickova H, Kornhuber B, Schwabe D, and Doerr HW (1998). Persistent human cytomegalovirus infection induces drug resistance and alteration of programmed cell death in human neuroblastoma cells. *Cancer Res* **58**, 367–372.

[5] Cinatl J Jr, Kotchetkov R, Scholz M, Cinatl J, Vogel JU, Driever PH, and Doerr HW (1999). Human cytomegalovirus infection decreases expression of thrombospondin-1 independent of the tumor suppressor protein p53. *Am J Pathol* **155**, 285–292.

[6] Beck K, Meyer-Konig U, Weidmann M, Nern C, and Hufert FT (2003). Human cytomegalovirus impairs dendritic cell function: a novel mechanism of human cytomegalovirus immune escape. *Eur J Immunol* **33**, 1528–1538.

[7] Rosenthal LJ and Choudhury S (1993). Molecular aspects of human cytomegalovirus diseases. In Becker, Y, Darai, G, Huang, ES (Eds.), *Frontiers of Virology*. **Vol. 2** 412–436, Springer-Verlag, Berlin.

[8] Grody WW, Lewin KJ, and Naeim F (1988). Detection of cytomegalovirus DNA in classic and epidemic Kaposi's sarcoma by in situ hybridization. *Hum Pathol* **19**, 524–528.

[9] Cinatl J, Scholz M, Kotchetkov R, Vogel JU, and Doerr HW (2004). Molecular mechanisms of the modulatory effects of HCMV infection in tumor cell biology. *Trends Mol Med* **10**, 19–23.

[10] Blaheta RA, Hundemer M, Mayer G, Vogel JU, Kornhuber B, Cinatl J, Markus BH, Driever PH, and Cinati J Jr (2002). Expression level of neural cell adhesion molecule (NCAM) inversely correlates with the ability of neuroblastoma cells to adhere to endothelium *in vitro*. *Cell Commun Adhes* **9**, 131–147.

[11] Cinatl J Jr, Vogel JU, Cinatl J, Weber B, Rabenau H, Novak M, Kornhuber B, and Doerr HW (1996). Long-term productive human cytomegalovirus infection of a human neuroblastoma cell line. *Int J Cancer* **65**, 90–96.

[12] Cinatl J Jr, Cinatl J, Radsak K, Rabenau H, Weber B, Novak M, Benda R, Kornhuber B, and Doerr HW (1994). Replication of human cytomegalovirus in a rhabdomyosarcoma cell line depends on the state of differentiation of the cells. *Arch Virol* **138**, 391–401.

[13] Bereiter-Hahn J, Fox CH, and Thorell B (1979). Quantitative reflection contrast microscopy of living cells. *J Cell Biol* **82**, 767–779.

[14] Gingell D and Todd J (1979). Interference reflection microscopy: a quantitative theory for image interpretation and its application to cell–substratum separation measurement. *Biophys J* **26**, 507–526.

[15] Blaheta RA, Kronenberger B, Woitaschek D, Weber S, Scholz M, Schuldes H, Encke A, and Markus BH (1998). Development of an ultrasensitive *in vitro* assay to monitor growth of primary cell cultures with reduced mitotic activity. *J Immunol Methods* **211**, 159–169.

[16] Edvardsen K, Weiching CH, Rucklidge G, Walsh FS, Öbrink B, and Bock E (1993). Transmembrane neural cell-adhesion molecule (NCAM), but not glycosyl-phosphatidylinositol–anchored NCAM, down-regulates secretion of matrix metalloproteinases. *Proc Natl Acad Sci USA* **90**, 11463–11467.

[17] Shinmura Y, Kosugi I, Kaneta M, and Tsutsui Y (1999). Migration of virus-infected neuronal cells in cerebral slice cultures of developing mouse brains after *in vitro* infection with murine cytomegalovirus. *Acta Neuropathol (Berl)* **98**, 590–596.

[18] Shinmura Y, Kosugi I, Aiba-Masago S, Baba S, Yong LR, and Tsutsui Y (1997). Disordered migration and loss of virus-infected neuronal cells in developing mouse brains infected with murine cytomegalovirus. *Acta Neuropathol (Berl)* **93**, 551–557.

[19] Streblow DN, Soderberg-Naucler C, Vieira J, Smith P, Wakabayashi E, Ruchti F, Mattison K, Altschuler Y, and Nelson JA (1999). The human cytomegalovirus chemokine receptor US28 mediates vascular smooth muscle cell migration. *Cell* **99**, 511–520.

[20] Zhou YF, Yu ZX, Wanishsawad C, Shou M, and Epstein SE (1999). The immediate early gene products of human cytomegalovirus increase vascular smooth muscle cell migration, proliferation, and expression of PDGF beta-receptor. *Biochem Biophys Res Commun* **256**, 608–613.

[21] Scholz M, Blaheta RA, Wittig B, Cinatl J, Vogel JU, Doerr HW, and Cinatl J Jr (2000). Cytomegalovirus-infected NB cells exhibit augmented invasiveness mediated by beta1alpha5 integrin (VLA-5). *Tissue Antigens* **55**, 412–421.

[22] Owens GC, Orr EA, DeMasters BK, Muschel RJ, Berens ME, and Kruse CA (1998). Overexpression of a transmembrane isoform of neural cell adhesion molecule alters the invasiveness of rat CNS-1 glioma. *Cancer Res* **58**, 2020–2028.

[23] Prag S, Lepekhin EA, Kolkova K, Hartmann-Petersen R, Kawa A, Walmod PS, Belman V, Gallagher HC, Berezin V, Bock E, and Pedersen N (2002). NCAM regulates cell motility. *J Cell Sci* **115**, 283–292.

[24] Edvardsen K, Pedersen P-H, Bjerkvig R, Hermann GG, Zeuthen J, Laerum OD, Walsh FS, and Bock E (1994). Transfection of glioma cells with the neural-cell adhesion molecule NCAM: effect on glioma cell invasion and growth *in vivo*. *Int J Cancer* **58**, 116–122.

[25] Huerta S, Srivatsan ES, Venkatesan N, Peters J, Moatamed F, Renner S, and Livingston EH (2001). Alternative mRNA splicing in colon cancer causes loss of expression of neural cell adhesion molecule. *Surgery* **130**, 834–843.

[26] Roesler J, Srivatsan E, Moatamed F, Peters J, and Livingston EH (1997). Tumor suppressor activity of neural cell adhesion molecule in colon carcinoma. *Am J Surg* **174**, 251–257.

[27] Sampson-Johannes A, Wang W, and Shtivelman E (1996). Colonization of human lung grafts in SCID-hu mice by human colon carcinoma cells. *Int J Cancer* **65**, 864–869.

[28] Cavallaro U, Niedermeyer J, Fuxa M, and Christofori G (2001). N-CAM modulates tumour-cell adhesion to matrix by inducing FGF-receptor signalling. *Nat Cell Biol* **3**, 650–657.

[29] Perl AK, Dahl U, Wilgenbus P, Cremer H, Semb H, and Christofori G (1999). Reduced expression of neural cell adhesion molecule induces metastatic dissemination of pancreatic beta tumor cells. *Nat Med* **5**, 286–291.

[30] Tezel E, Kawase Y, Takeda S, Oshima K, and Nakao A (2001). Expression of neural cell adhesion molecule in pancreatic cancer. *Pancreas* **22**, 122–125.

[31] Akeson R and Bernards R (1990). N-myc down regulates neural cell adhesion molecule expression in rat neuroblastoma. *Mol Cell Biol* **10**, 2012–2016.

[32] Judware R and Culp LA (1995). Over-expression of transfected *N-myc* oncogene in human SKNSH neuroblastoma cells down-regulates expression of beta 1 integrin subunit. *Oncogene* **11**, 2599–2607.

[33] Kotchetkov R, Cinatl J, Blaheta R, Vogel JU, Karaskova J, Squire J, HernaizDriever P, Klingebiel T, and Cinatl J Jr (2003). Development of resistance to vincristine and doxorubicin in neuroblastoma alters malignant properties and induces additional karyotype changes: a preclinical model. *Int J Cancer* **104**, 36–43.

[34] Kaghad M, Bonnet H, Yang A, Creancier L, Biscan JC, Valent A, Minty A, Chalon P, Lelias JM, Dumont X, Ferrara P, McKeon F, and Caput D (1997). Monoallelically expressed gene related to p53 at 1p36, a region frequently deleted in neuroblastoma and other human cancers. *Cell* **90**, 809–819.

[35] Melino G, De Laurenzi V, and Vousden KH (2002). p73: friend or foe in tumorigenesis. *Nat Rev Cancer* **2**, 605–615.

[36] Douc-Rasy S, Barrois M, Echeynne M, Kaghad M, Blanc E, Raguenez G, Goldschneider D, Terrier-Lacombe MJ, Hartmann O, Moll U, Caput D, and Benard J (2002). DeltaN-p73alpha accumulates in human neuroblastic tumors. *Am J Pathol* **160**, 631–639.

[37] Casciano I, Mazzocco K, Boni L, Pagnan G, Banelli B, Allemanni G, Ponzoni M, Tonini GP, and Romani M (2002). Expression of DeltaNp73 is a molecular marker for adverse outcome in neuroblastoma patients. *Cell Death Differ* **9**, 246–251.

[38] De Laurenzi V, Raschella G, Barcaroli D, Annicchiarico-Petruzzelli M, Ranalli M, Catani MV, Tanno B, Costanzo A, Levrero M, and Melino G (2000). Induction of neuronal differentiation by p73 in a neuroblastoma cell line. *J Biol Chem* **275**, 15226–15231.

[39] Zhu X, Wimmer K, Kuick R, Lamb BJ, Motyka S, Jasty R, Castle VP, and Hanash SM (2002). N-myc modulates expression of p73 in neuroblastoma. *Neoplasia* **4**, 432–439.

[40] Allart S, Martin H, Detraves C, Terrasson J, Caput D, and Davrinche C (2002). Human cytomegalovirus induces drug resistance and alteration of programmed cell death by accumulation of deltaN-p73alpha. *J Biol Chem* **277**, 29063–29068.